Paper No. 1772. (quote when citing this article)
Eleventh World Conference on Earthquake Engineering
ISBN: 0 08 042822 3

RESPONSE SPECTRA OF GROUND MOTION ABOVE EARTHQUAKE FAULT

Hiroshi DOHI[1], Masahiro KAWANO[2] and Satoshi MATSUDA[3]

1) Research and Development Department, NTT Power and Building facilities Inc.
3-9-11, Midori-Cho, Musashino-Shi, Tokyo 180, JAPAN
2) Department of Architectural Engineering, Faculty of Engineering, Kyoto University
Yoshida Honmachi, Sakyo-Ku, Kyoto-Shi, Kyoto 606, JAPAN
3) Department of Architecture Faculty of Engineering, Kansai University
3-3-35, Yamate-Cho, Suita-Shi, Osaka 564, JAPAN

ABSTRACT

Hanshin area including Kobe and Osaka suffered a tremendous damage by the Hyogo-ken Nanbu Earthquake of January 17, 1995. The big earthquake records were obtained in Kobe, because Kobe is located just above the earthquake fault. However, there were many severely damaged and slightly damaged structures in this area. Therefore, it is an important problem to investigate what are the major factors to produce such differences of damages on structures. In this study, the ground motion model above the fault plane is presented by making use of wave propagation theory and source dynamics. Through the post prediction test for ground motion models of the three sites, the time histories and spectral characteristics and of observed ground motions, and structural responses are investigated for some causative factors associated with source, site and path.

KEYWORDS

Ground motion above earthquake fault; wave propagation theory; source dynamics; Green's function; source function; multi-layered half-space; random medium

INTRODUCTION

Hanshin area including Kobe and Osaka suffered a tremendous damage by the Hyogo-ken Nanbu Earthquake of January 17, 1995. The big earthquake records were obtained at many sites in Kobe, because Kobe is located just above the earthquake fault. However, there were many severely damaged and slightly damaged structures in this area. It is considered that the ground motions of the Hyogo-ken Nanbu Earthquake of January 17, 1995 are strongly conditioned by not only the site amplification but also the source dynamics, because the rupture on earthquake fault occurred just under sites. Therefore, it is an important problem to investigate what are the major factors to produce such differences of damages on structures. The purpose of this study is to present the ground motion model in the very near field by making use of wave propagation theory and source dynamics and to investigate structural responses for some causative factors associated with source, site and path. The geological profiles in and around Kobe take fan-shape, which consists of thicker surface layer with irregular boundary overlying basement bedrock in the north to the south direction. The soil sediment and geological structures from source to basement bedrock are investigated by the boring data, seismic velocities by PS logging and observed weak ground motions. It is very difficult to estimate rigorously the geological structure of actual three-dimensional sediment-filled basins. Therefore, in this study, the soil sediment and basement bedrock beneath each observation site in Kobe is idealized by the multi-layered half-space overlying a random medium. The Green's functions from source to the three sites are calculated exactly according to the geological data investigated. The source

Table 1 Fault parameters

Segment	lon.(deg)	lat.(deg)	depth(m)	strike(deg)	dip.(deg)
A	134.858	34.4959	0.0	N45E	82
B	135.028	34.6041	0.0	N53E	90
C	135.365	34.7957	0.0	N233E	85

(Sekiguchi *et al.*, 1995)

Table 2 Site locations

	lon.(deg)	lat.(deg)
Site 1 (Kobe univ.)	135.240	34.725
Site 2 (Kansai electric)	135.250	34.731
Site 3 (Matsumura corp.)	135.217	34.850

function is described through fitting the wave form function of ground motion model to the only NS component of ground motion observed at Site 1. The source function is used to present the ground motion models at Site 2 and Site 3. Then, the ground motions are theoretically estimated for Site 1, Site 2, and Site 3. Through the post prediction test for ground motion models of the three sites, the time histories and spectral characteristics and of observed ground motions, and structural responses of them are investigated for some causative factors associated with source, site and path.

THE HYOGO-KEN NANBU EARTHQUAKE DATA

Figure 1 shows the causative fault and the three observation sites in Kobe. The fault parameters are summarized in Table 1. The locations of the sites are listed in Table 2. The magnitude of the earthquake is estimated to be M=7.2. The hypocenter is situated at 34.593° north latitude and 135.035° east longitude and is at depth of 17.9km. The seismic moment is M0 = 2.5×10^{26} dyne•cm (Kikuchi, 1995). There are three major fault segments ,A,B and C as shown in Fig. 1. Sekiguchi, et al. (1995) estimated a slip distribution during rupture on fault surface from the inversion of earthquake records as shown in Fig. 2. In this study, the fault segments B and C, hatched in Fig. 2, are used to obtain synthetic ground motion, since the great seismic energy is radiated from the events on these segments. The seismic waves from the segments effectively characterize the ground motions in Kobe.

WAVE PROPAGATION PATH AND SITE EFFECT MODEL

The geological profiles in and around Kobe city take fan-shape, which consists of thicker surface layer with irregular boundary overlying basement bedrock in the north to the south direction. The soil sediment and geological structures from source to basement bedrock are investigated by the boring data, seismic velocities by PS logging and observed weak ground motions. It is very difficult to estimate rigorously the geological structure of actual three-dimensional sediment-filled basins. It is often pointed out that the one-dimensional soil sediment model predict successfully the direct phases of the ground motions in sedimentary basin (Scrivner and Helmberger, 1994) . Therefore, in this study, the soil sediment and basement bedrock beneath each observation site in Kobe is idealized by the multi-layered half-space overlying a random medium as shown in Fig. 3.

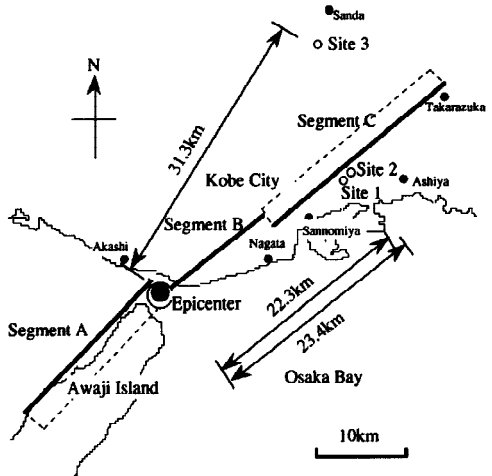

Fig. 1 Location of observation sites and epicenter

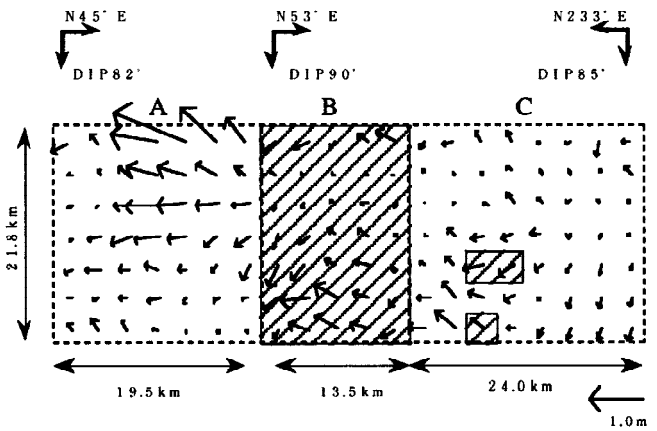

Fig. 2 Slip vector distribution on the fault surface (Sekiguchi *et al.*(1995))

Table 3 Geological data of soil sediment structure of observation sites

Table 3.1 Site 1

Depth H(m)	P-wave velocity Vp(m/sec)	S-wave velocity Vs (m/sec)	Density ρ (g/cm3)	Damping factor h(%)	
				Vp	Vs
10.45 ~ 11.75	490	240	1.968	1.0	1.0
11.75 ~ 16.0	700	340	1.968	1.0	1.0
16.0 ~ 20.8	1700	590	2.265	1.0	1.0
20.8 ~ 33.0	2050	850	2.086	1.0	1.0
33.0 ~ 40.45	2250	960	2.146	0.167	0.500
40.45 ~ 52.95	2850	1120	2.180	0.143	0.333
52.95 ~ 70.0	3100	1350	2.20	0.143	0.333
70.0 ~ 500.0	2950	1425	2.20	0.143	0.333
500.0 ~ 800.0	2800	1500	2.20	0.143	0.333
800.0 ~ 900.0	4250	2850	2.30	0.125	0.333
900.0 ~ 5000.0	5700	3200	2.45	0.100	0.200
5000.0 ~ 18000.0	6000	3460	2.80	0.038	0.083
18000.0 ~	6700	3870	3.00	0.029	0.063

Table 3.2 Site 2

Depth H(m)	P-wave velocity Vp(m/sec)	S-wave velocity Vs (m/sec)	Density ρ (g/cm3)	Damping factor h(%)	
				Vp	Vs
0.0 ~ 3.0	630	200	1.80	1.0	1.0
3.0 ~ 10.0	1000	300	2.00	1.0	1.0
10.0 ~ 14.0	1460	450	2.00	1.0	1.0
14.0 ~ 27.0	2130	450	2.10	1.0	1.0
27.0 ~ 33.0	2130	690	2.20	1.0	1.0
33.0 ~ 45.0	2130	450	2.10	1.0	1.0
45.0 ~ 70.0	2750	640	2.50	0.167	0.50
70.0 ~ 139.0	2750	780	2.60	0.167	0.50
139.0 ~ 150.0	2350	610	2.60	0.167	0.50
150.0 ~ 500.0	2575	1055	2.40	0.155	0.417
500.0 ~ 800.0	2800	1500	2.20	0.143	0.333
800.0 ~ 900.0	4250	2850	2.30	0.125	0.333
900.0 ~ 5000.0	5700	3200	2.45	0.100	0.200
5000.0 ~ 18000.0	6000	3460	2.80	0.038	0.083
18000.0 ~	6700	3870	3.00	0.029	0.063

Table 3.3 Site 3

Depth H(m)	P-wave velocity Vp(m/sec)	S-wave velocity Vs (m/sec)	Density ρ (g/cm3)	Damping factor h(%)	
				Vp	Vs
0.0 ~ 5.0	370	180	1.60	1.0	1.0
5.0 ~ 8.0	1070	230	1.80	1.0	1.0
8.0 ~ 12.0	1940	390	2.10	1.0	1.0
12.0 ~ 15.0	1940	910	2.20	0.167	0.50
15.0 ~ 18.0	2500	1110	2.20	0.167	0.50
18.0 ~ 27.0	2170	980	2.20	0.167	0.50
27.0 ~ 30.0	2170	1000	2.20	0.167	0.50
30.0 ~ 500.0	2470	1250	2.20	0.155	0.417
500.0 ~ 800.0	2800	1500	2.20	0.143	0.333
800.0 ~ 900.0	4250	2850	2.30	0.125	0.333
900.0 ~ 5000.0	5700	3200	2.45	0.100	0.200
5000.0 ~ 18000.0	6000	3460	2.80	0.038	0.083
18000.0 ~	6700	3870	3.00	0.029	0.063

The propagation spectra of seismic wave motion is considered to be mainly governed with the amplification characteristics of surface layer and the multiple scattering characteristics in the heterogeneous earth structure from source to site (Aki, 1984). It would be reasonable to present the wave propagation path from source to site by the multi-layered half-space which consists of surface layer overlying a semi-infinite random medium (Kawano, 1976, 1993 ; Kawano *et al.*,1995; Sato, 1984). The three observation sites among many sites are selected to obtain synthetic ground motions, since the shallow soil sediment structures at those sites were investigated relatively in detail on the basis of the boring data and seismic velocities by PS logging. The rough profiles of shear wave velocities in the deeper soil structure including basement bedrock of the Kobe city was investigated by Iwata *et al.* (1995).
The geological data under the three sites are summarized in Tables 3.1, 3.2 and 3.3. Those data are used to constitute the refined wave propagation path and site effects model in calculating Green's functions of the ground motion. Figure 3 shows amplification ratio spectra of the three sites which are estimated by one-dimensional soil sediment models. The spectra have large component at the period about 2.5 sec and small component at the period about 1.2 sec in common, which depend on the deeper soil structure.

MODELING GROUND MOTION

The ground motion model is presented on the basis of wave motion propagation in the multi-layered half-space and the simple source function. For the estimation of the Green's functions of the three sites 1, 2 and 3, the fault surface with length L and width W is divided into N small elements, called fault element as shown in Fig. 4. The seismic waves are radiated from the subevents on the N fault elements.

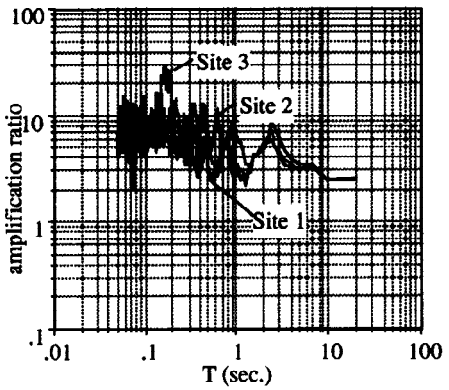

Fig. 3 Amplification ratios of sites (by 1D soil sediment model)

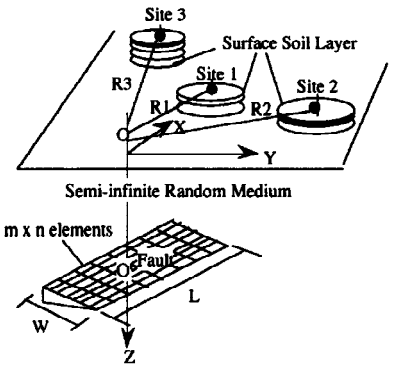

Fig. 4 Geometric relation between causative fault and sites

The rupture process on the fault surface is reduced to the source function which is expressed by the dynamic behaviors of mass-spring system on the rough surface (Ben-Menahem, 1976). By using this function, the source spectrum of the subevent at the kth fault element is assumed to be

$$\Delta u^{0}_{(k)}(x,\omega) = \frac{\Delta\bar{u}_{(k)}}{\sqrt{(\omega\tau_k)^2+1}} \frac{\sin(\omega T_k/2)}{\omega T_k/2} \exp\left[-i\left\{\omega x/V_{rk}+\tan^{-1}(\omega\tau_k)-\pi/2\right\}\right] \tag{1}$$

$$M_{(k)pq}(\omega) = R_{pq} M_{0(k)}(\omega) \qquad M_{0(k)}(\omega) = \mu \int\int_{\Sigma_{\xi k}} \Delta u^{0}_{(k)}(\xi, \omega)\, d\Sigma_{\xi k}(\xi)$$

$$T_k = L_e / V_{rk}, \quad L = \sqrt{N}\, L_e, \quad W = \sqrt{N}\, W_e$$

where $\Delta\bar{u}_{(k)}$, R_{pq}, $M_{0(k)}(\omega)$, μ, T_k, τ_k, and V_{rk} are slip displacement, radiation pattern, seismic moment, shear rigidity, rupture time, rise time, and rupture velocity at the kth fault element $\Sigma_{\xi k}$, ω is frequency. L_e and W_e are length and width of fault element.

The rupture occurs at each fault element and propagates bidirectionally (Sekiguchi *et al.*,1995). The high frequency components included in the ground motion model is governed by the rise time at the least fault element.

The large earthquake is composed of smaller earthquakes for the subevents on the fault surface. There are two physical properties in adding the smaller earthquakes from some areas of the fault surface. The subevent spectra add coherently at the lower frequencies and add incoherently at the higher frequencies. As a result, the spectra of the large event is flat at the lower frequencies and is proportional to the square root of the spectra at the higher frequencies. The large event spectrum is equal to the sum of the subevent spectra. According to the above scaling law, the source spectra of the large event is shown to be (Joyner and Boore, 1986)

$$S(\omega) = E\{(\sum_{j=1}^{N} \kappa S_{ej}(\omega) e^{-i\omega t_j})(\sum_{k=1}^{N} \kappa S^{*}_{ek}(\omega) e^{i\omega t_k})\} \tag{2}$$

where $S_{ej}(\omega) = M_{0(j)}(\omega)$ is the source spectrum of the subevent at the jth fault element, * denotes the complex conjugate. For the ω square spectrum of the earthquake, N and κ in equation (1) are described as

$$N = (M_0 / M_{0e})^{\frac{4}{3}}, \quad \kappa = (M_0 / M_{0e})^{-\frac{1}{3}}, \quad M_{0e} = M_0\, n^{-\frac{3}{2}}, \quad N = n^2 \tag{3}$$

where M_0 and M_{0e} are seismic moments of the large event and the subevent. The scaling law needs the great number summation of smaller earthquakes to be equal to the large earthquake. This number is determined to maintain self-similarity in spectral shape between the subevent and the large event based on ω-squared scaling relation (Joyner and Boore, 1986).

The ground motion model is expressed by summation of wave motions radiated at the times when the rupture front reaches the fault elements as follows;

$$Y_n(x; t) = \sum_{k=1}^{N} \int_0^t M_{(k)pq}(\xi, \tau)\, \partial G_{np}(x, t-\tau; \xi, 0)/\partial\xi_q\, d\tau \tag{4}$$

where $G_{np}(x, t-\tau; \xi, 0)$ is the nth component of displacement at position x and time $t-\tau$ caused by an instantaneous force of unit amplitude applied in the p direction at ξ and time $t=0$. The Green's function from source to each site are calculated for the points on the fault surface using wave number integral method (Luco and Apsel, 1983).

NUMERICAL RESULTS AND DISCUSSION

To investigate the clear correspondence between observed ground motions and the ground motion model presented here, the post prediction test is conducted for the Hyogo-ken Nanbu Earthquake of January 17,1995. The source slip distribution on the fault surface is estimated by Sekiguchi *et al.* (1995). The other parameters such as rise time and rupture velocity on each fault element are described through fitting the wave form function of ground motion model to the only NS component of ground motion observed at Site 1. The one source function is determined by the above procedure and is used to present the ground motion model at the Site 2 and Site 3.

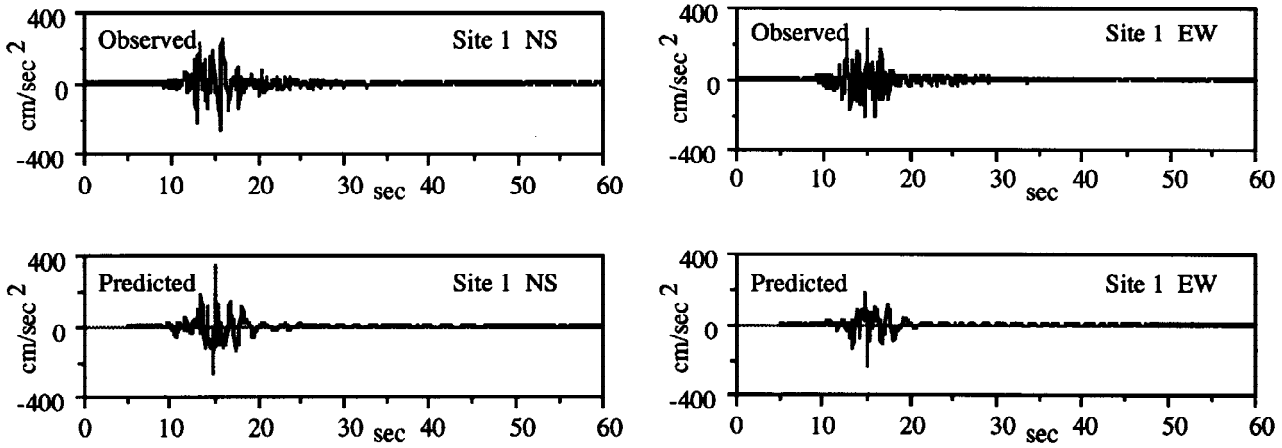

Fig. 5 Comparison of observed and predicted acceleration wave forms at Site 1

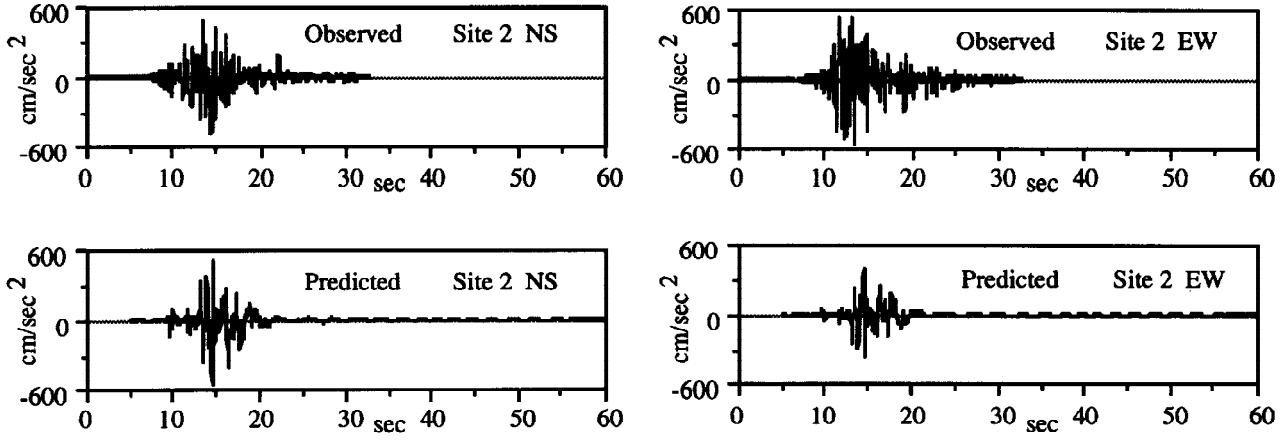

Fig. 6 Comparison of observed and predicted acceleration wave forms at Site 2

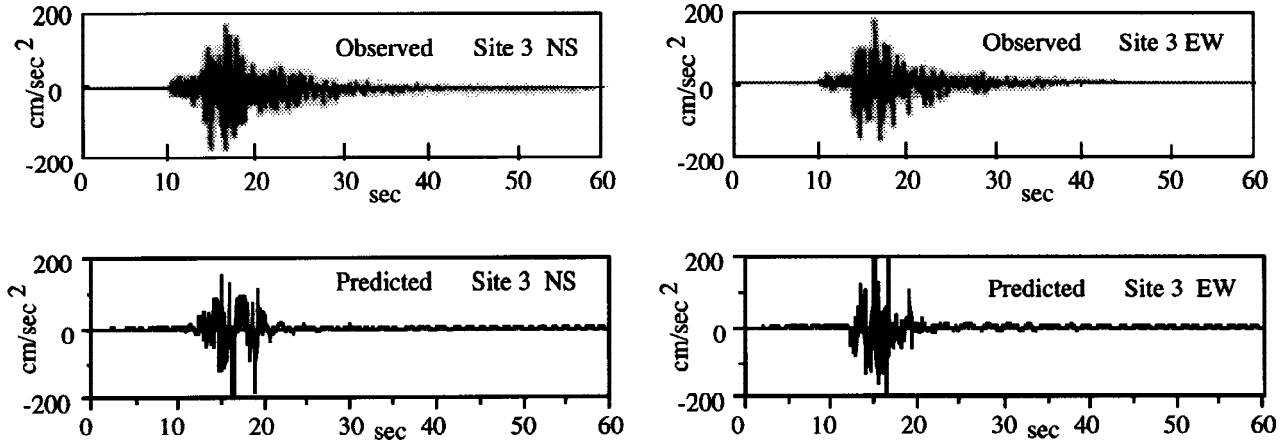

Fig. 7 Comparison of observed and predicted acceleration wave forms at Site 3

Then, the ground motions of NS and EW components are estimated for the Site 1, Site 2, and Site 3. As the soil sediment model and the source model are clearly described at this stage, it is possible to discuss the characteristics of observed ground motions and structural responses. They are compared with the corresponding components of the observed ground motions as shown in Figs. 5, 6 and 7. Though the segments B and C are used to provide the ground motion model, they are very similar each other in the peak amplitude and the main portions of the time histories of ground motions. Therefore, the fault segments B and C contribute significantly to the constitute of the characteristics of the ground motions. The duration times of ground motions at Site 1 and Site 2 in the very near field, are shorter and the peak amplitudes are bigger than the corresponding ones at Site 3. Figures 8 and 9 show the comparison of the predicted and observed velocity response spectra for Site 1 and Site2. Fairly good agreement between the predicted and observed response spectra is obtained in wide period range. It is found that the spectral characteristics of surface soil sediment layer is not always emphasized for the ground motion in the very near field. Thereby, when the periods of direct phases from the source region coinside with those of surface soil sediment layer, the great energy from the source would transmit a structural system on and in the soil ground. Even though the observed ground motions have much spectra component around 1.2 sec, the amplification ratio spectra of soil sediment model for the three sites have very small component at the same period. The more precise estimation of the deeper soil structure would improve the difference in the response spectra around 1.2 sec.

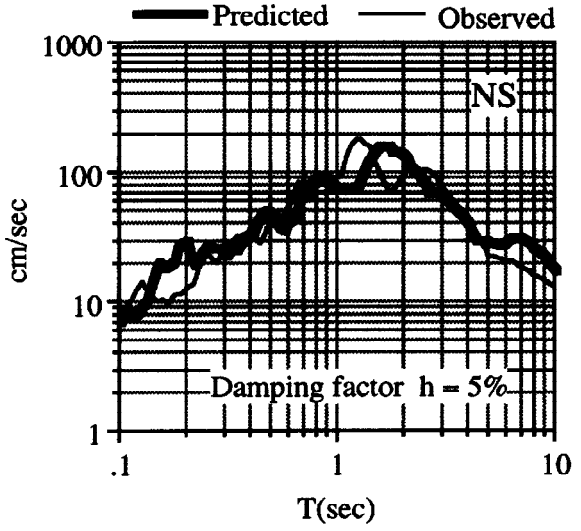

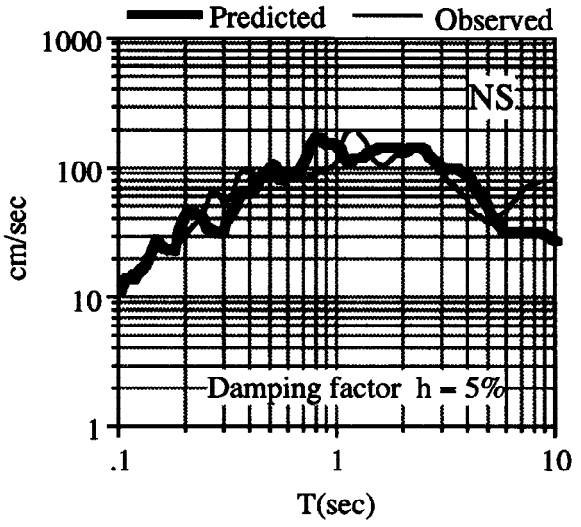

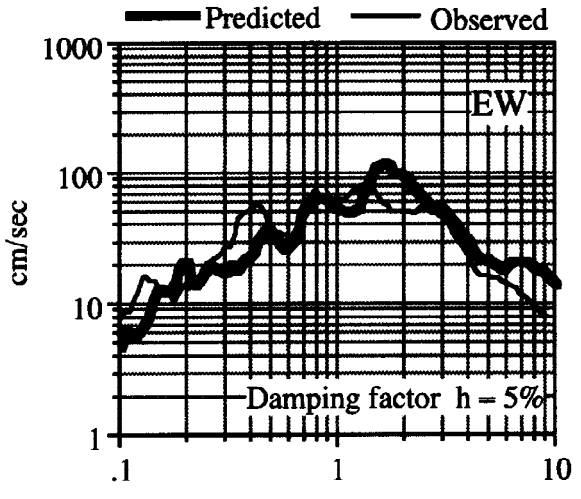

Fig. 8 Site 1

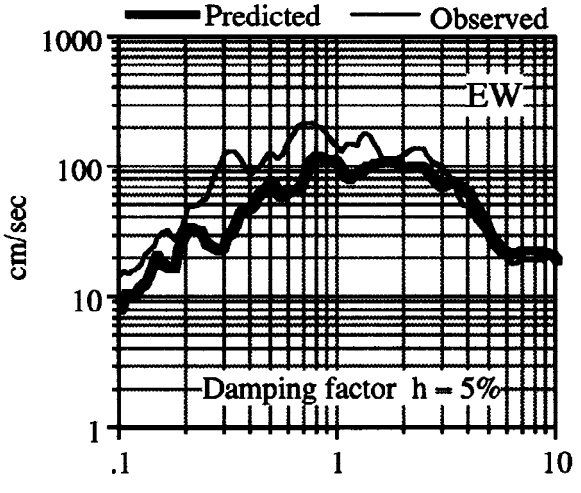

Fig. 9 Site 2

Comparison of observed and predicted velocity response spectra

CONCLUSION

The ground motion model has been presented for the estimation of structural response of the site above the fault plane in Kobe and tested against the earthquake ground motions at the three observation sites for the Hyogo-ken Nanbu Earthquake of January 17, 1995. The ground motions has been theoretically expressed by the Green's functions and the one source function which is described by the only NS component of the wave form at Site 1. The theoretical ground motions agree well with the observed ones in the peak amplitude, the main portion of time histories, and velocity response spectra over wide period range although the fault segments B and C are used to provide theoretical ground motions. The time histories and spectra of the ground motions in the very near field are affected by the source characteristics and wave propagation from source to site so that spectral characteristics of surface soil sediment layer do not always reflect strongly on the ground motion in the very near field. Thereby, when the periods of direct phases from the source region coinside with those of surface soil sediment layer, the great energy from the source would transmit a structural system on and in the soil ground.

ACKNOWLEDGMENTS

The authors wish to thank Kobe University, Kansai Electric Power Co. Inc., and Matumura Construction for providing us with their strong ground motion data from Hyogo-ken Nanbu Earthquake of January 17, 1995.

REFERENCES

Aki, K. (1984): Prediction of Strong Motion using Physical Models of Earthquake Faulting, *Proc. of 8th WCEE*, 2, .433-440.

Ben-Menahem, A. (1976): The Role of the Shear Mach Number in Earthquake Source Dynamics, *Bull. Seism. Soc. Am.*, 66, 1787-1799.

Iwata, T., K. Hatayama, H. Kawase and K. Irikura (1995): Site Amplification of Ground Motions during Aftershocks of the 1995 Hyogoken-nanbu Earthquake in Severely Damaged Zone - Array Observation of Ground Motions at Higashinada Ward, Kobe City, Japan -, Submitted to *J. Phys. Earth.*

Joyner, W.B. and D. M. Boore (1986): Earthquake Source Mechanics, *Maurice Ewing Ser. 6, edited by Das. S., and J. Boatwright,* 269-274.

Kawano, M. (1993): Earthquake Motion and Ground Conditions, *AIJ,* 79-95.

Kawano, M., H. Dohi and S. Matsuda (1995) : A Study of Seismic Intensity in the Kanto Plain by Ground Motion Model, *Proc. of 5th Intr. Conf. Microzonation,* 1059-1066.

Kikuchi, M. (1995) : The Hyogo-ken Nanbu Earthquake of 1995, *Chikyu Monthly,* Extra No.13, 47-53.

Kobori, T., Y.Takeuchi and M. Kawano (1977): On some Properties of Wave Propagation in a Continuous Random Media, *Proc. of 6th WCEE*, 605-610.

Luco J. E. and R. J. Apsel (1983): On the Green's Functions for a Layered Half-Space, Part I, *Bull. Seism. Soc. Am.*, 73, 909-929.

Sato, H. (1984): Attenuation and Envelope Formation of Three-Component Seismograms of Small Local Earthquake in Randomly Inhomogeneous Lithosphere, *J. Geophys. Res.*, 89, 1221-1241.

Scrivner, C.W. and D.V. Helmberger (1994): Seismic Waveform Modeling in the Los Angeles Basin, *Bull. Seism. Soc. Am.*, 84, 1310-1326.

Sekiguchi, H., K. Irikura, T. Iwata, Y. Kakei and M. Hoshiba (1995) : Minute Locationing of Fault Planes and Source Process of the 1995 Hyogo-ken Nanbu(Kobe), Japan Earthquake from the Waveform Inversion of Strong Ground Motion, Submitted to *J. Phys. Earth.*